

A NEW DIVERGENCE-FREE INTERPOLATION OPERATOR WITH APPLICATIONS TO THE DARCY–STOKES–BRINKMAN EQUATIONS*

XUEJUN XU[†] AND SHANGYOU ZHANG[‡]

Abstract. A new local interpolation operator, preserving the divergence, is constructed explicitly for the Hsieh–Clough–Tocher divergence-free element. A divergence-free finite element method is applied to the Darcy–Stokes–Brinkman flow in a mixed region of both free and porous media. The method is of optimal order as well for the Darcy flow as for the Stokes flow (which is not the case for most other finite elements). Compared to the existing nonconforming elements, the divergence-free element method provides a continuous solution for the velocity which is also an orthogonal projection within a Hilbert subspace of the true velocity. Numerical tests supporting the theory are presented.

Key words. mixed finite element, Stokes equations, Darcy’s law, Brinkman equations, divergence-free element

AMS subject classifications. 65M60, 65N30, 76M10, 76D07

DOI. 10.1137/090751049

1. Introduction. We consider a model Darcy–Stokes–Brinkman mixed flow problem (cf. [10, 19]): Find the velocity \mathbf{u} and the pressure p such that

$$(1.1) \quad \begin{cases} -\epsilon^2 \Delta \mathbf{u} + \mathbf{u} + \nabla p = \mathbf{f} & \text{in } \Omega, \\ \operatorname{div} \mathbf{u} = g & \text{in } \Omega, \\ \mathbf{u} \cdot \mathbf{n} = 0 \text{ and } \epsilon \mathbf{u} \cdot \mathbf{t} = \mathbf{0} & \text{on } \partial\Omega, \end{cases}$$

where Ω is a bounded polygonal domain in \mathbf{R}^2 , \mathbf{n} and \mathbf{t} denote the outward normal and tangential unit vectors along the boundary $\partial\Omega$, respectively, and $\int_{\Omega} g = 0$. When $\epsilon = 0$, (1.1) becomes the Darcy’s law for porous medium flow. When $\epsilon = 1$, (1.1) is a form of Stokes equations, modeling free fluid flow. When the singular perturbation parameter ϵ varies between 0 and 1 in the domain, the partial differential equations (1.1) change the type. The Darcy–Stokes–Brinkman equations can be applied to fuel cell dynamics, for example, which model the flow of gas and water in a multidomain by one set of equations on a single domain, cf. [11, 19].

As pointed out in [10], most traditional $\mathbf{H}^{\operatorname{div}}$ mixed elements for second order elliptic equations (when $\epsilon = 0$) and \mathbf{H}^1 mixed elements for the incompressible fluids and nearly incompressible materials (when $\epsilon = 1$) do not work for ϵ both close to 0 and 1. In most mixed finite elements for the Stokes equations, to satisfy the inf-sup condition, the finite element space for the velocity is chosen too large in the sense that (many) finite element functions \mathbf{v}_h in the velocity space \mathbf{V}_h exist such that $\|\operatorname{div} \mathbf{v}_h\|_{L^2} \neq 0$ but

$$(1.2) \quad (\operatorname{div} \mathbf{v}_h, q_h) = 0$$

*Received by the editors February 27, 2009; accepted for publication (in revised form) December 22, 2009; published electronically March 10, 2010. This work was supported by State Key Laboratory of Scientific and Engineering Computing, CAS.

<http://www.siam.org/journals/sisc/32-2/75104.html>

[†]LSEC, Institute of Computational Mathematics, Chinese Academy of Sciences, P.O. Box 2719, Beijing 100080, China (xxj@lsec.cc.ac.cn). The work of this author partially supported by the special funds for major state basic research projects (973) under 2005CB321701 and NSF of China (10731060).

[‡]Department of Mathematical Sciences, University of Delaware, Newark, DE 19716 (szhang@udel.edu).

for all q_h in the finite element pressure space P_h . In this case, the nondivergence-free part of the finite element solution \mathbf{u}_h is not controlled by the second equation of (1.1) due to (1.2) and also is not controlled well by the first equation in (1.1) in the case $\epsilon = 0$. It is controlled only by the lower-order term in the first equation of (1.1). This results in $\|\operatorname{div} \mathbf{u}_h - g\|_{L^2} \not\rightarrow 0$ and even $\|\operatorname{div} \mathbf{u}_h\|_{L^2} \rightarrow \infty$, usually. Two such examples are provided in [10]. On the other side, in most $\mathbf{H}^{\operatorname{div}}$ -element methods for the Darcy's law, the finite element velocity space may not be an \mathbf{H}^1 space, neither an \mathbf{H}^1 -nonconforming space. It is not clear yet which of them may work for the Stokes equations. The most popular $\mathbf{H}^{\operatorname{div}}$ -element, the lowest order Raviart–Thomas element, for example, is constructed with zero curl. Then it would not work for the Stokes equations. This is shown numerically in [10].

For a pair of mixed-element spaces to work uniformly for the problem (1.1) with $\epsilon \in [0, 1]$, a compatible condition is, pointed out by Mardal, Tai, and Winther in (3.4) of [10] (also see (4.2) in this manuscript), in addition to the standard inf-sup condition (2.6) below,

$$(1.3) \quad \|\operatorname{div} \mathbf{v}_h\|_{L^2} \leq C \|\mathbf{v}_h\|_{\mathbf{L}^2}$$

for all \mathbf{v}_h satisfying (1.2). For all \mathbf{H}^1 -conforming, divergence-free elements, such as the Scott–Vogelius element [14], (1.3) holds trivially as the left-hand side is 0. In such a case, we have

$$(1.4) \quad \operatorname{div} \mathbf{V}_h = P_h.$$

Of course, the div in (1.4) can be interpreted in a weak sense; i.e., div is a discrete divergence operator. In fact, the few element pairs constructed so far [10, 19] all satisfy (1.4) for the Darcy–Stokes–Brinkman system (1.1). But they all are \mathbf{H}^1 -nonconforming elements.

For the Stokes or Navier–Stokes equations, rewritten in variational forms, the primitive unknowns, the velocity and the pressure, belong to Sobolev spaces \mathbf{H}^1 and L^2 , respectively. Naturally, a finite element method would be the P_k - P_{k-1}^{dc} element, which approximates the velocity in an \mathbf{H}^1 -subspace of continuous piecewise P_k polynomials and approximates the pressure in an L^2 -subspace of discontinuous P_{k-1} polynomials. This is a truly conforming element as the incompressibility condition is satisfied pointwise, and the discrete solution for the velocity is a projection within the space of divergence-free functions. We call such \mathbf{H}^1 finite elements divergence-free elements. A fundamental study on the method was done by Scott and Vogelius [14, 15] showing that the method is stable and consequently of the optimal order on 2D triangular grids for any $k \geq 4$, provided the grids have no nearly-singular vertex. Some other divergence-free elements are also discovered, cf. [1, 3, 4, 12, 20, 21, 22]. To be a divergence-free element, the necessary and sufficient condition is (1.4). In principle, all divergence-free elements would approximate the solutions of the Darcy–Stokes–Brinkman system in optimal order, uniformly for all $\epsilon \in [0, 1]$. In this work, however, we analyze only one type of divergence-free element, the 2D P_2 Hsieh–Clough–Tocher divergence-free element. This element was analyzed by Qin and shown to be stable for the Stokes equations in an unpublished work [12]. Nevertheless, our analysis is not based on Qin's work. We construct a new divergence-preserving interpolation operator \mathbf{I}_h , extending the Scott–Zhang operator [16]. Here the divergence-preserving is meant “pointwise” in the following sense, noting that $P_h = \operatorname{div} \mathbf{V}_h$ in (1.4),

$$(1.5) \quad P_0 \operatorname{div} \mathbf{u} = \operatorname{div} \mathbf{I}_h \mathbf{u},$$

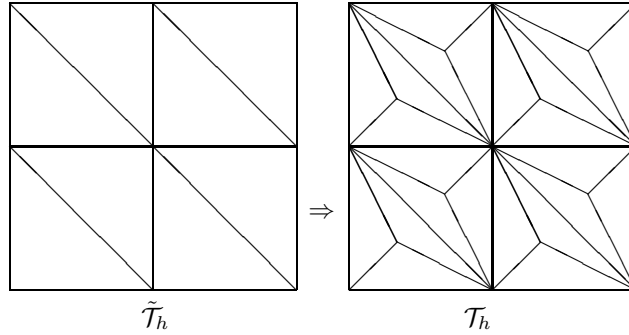


FIG. 1. A uniform triangulation \tilde{T}_h splits into a Hsieh-Clough-Tocher grid T_h .

where P_0 is the L_2 -orthogonal projection operator to the image space of divergence of discrete velocity space. In particular, $\text{div } \mathbf{I}_h \mathbf{u} = 0$ if $\text{div } \mathbf{u} = 0$. Previously, such operators were constructed by Girault and Scott [9], and some others [10, 19], for some finite elements but not for divergence-free elements. A divergence-preserving operator would imply the inf-sup condition for the finite element pair (\mathbf{V}_h, P_h) . With this divergence-preserving operator, the uniform convergence for (1.1) by the P_2 Hsieh-Clough-Tocher divergence-free element would be deduced. Therefore, we reproduce Qin's result [12] as a byproduct. Using the same technique, one can construct divergence-preserving operators for higher-order Hsieh-Clough-Tocher divergence-free elements on triangular grids, for example, the P_3 HCT element in [12], and for the P_k HCT divergence-free elements on tetrahedral grids for any $k \geq 3$, cf. [20]. But it seems this kind of construction would be possible only for such few macroelements.

2. The divergence-free element. Multiplying the Darcy-Stokes-Brinkman equations (1.1) by test functions and integrating by parts, the following variational form for the problem is derived: Find $\mathbf{u} \in \mathbf{V}$ and $p \in L_0^2(\Omega)$ such that

$$(2.1) \quad \begin{aligned} a_\epsilon(\mathbf{u}, \mathbf{v}) - (p, \text{div } \mathbf{v}) &= (\mathbf{f}, \mathbf{v}) \quad \forall \mathbf{v} \in \mathbf{V}, \\ (q, \text{div } \mathbf{u}) &= (g, q) \quad \forall q \in L_0^2(\Omega), \end{aligned}$$

where Ω is a 2D Lipschitz, polygonal domain with an outward normal vector \mathbf{n} ,

$$\mathbf{V} = \begin{cases} \mathbf{H}_0^1(\Omega) = H_0^1(\Omega)^d, & d = 2, 3, & \text{if } \epsilon > 0, \\ \mathbf{H}_0^{\text{div}}(\Omega) = \{ \mathbf{v} \in L^2(\Omega)^d \mid \text{div } \mathbf{v} \in L^2(\Omega), \mathbf{n} \cdot \mathbf{v} = 0 \}, & \text{if } \epsilon = 0, \end{cases}$$

$H_0^1(\Omega)$ is the Sobolev space with 0 trace on $\partial\Omega$, $L_0^2(\Omega)$ is the space of square integrable functions with mean $\int_\Omega (\cdot) \, d\mathbf{x} = 0$, and

$$a_\epsilon(\mathbf{u}, \mathbf{v}) = \epsilon^2 \int_\Omega \nabla \mathbf{u} \cdot \nabla \mathbf{v} \, d\mathbf{x} + (\mathbf{u}, \mathbf{v}), \quad (\mathbf{u}, \mathbf{v}) = \int_\Omega \mathbf{u} \mathbf{v} \, d\mathbf{x}.$$

The problem (2.1) is well posed (cf. [10, 13]) when $\epsilon \in [0, 1]$.

Let Ω be triangulated into quasiuniform grids \tilde{T}_h (cf. [7]) of triangles, with a grid size h . We consider one type of divergence-free elements. The theory established here would be generalized to all divergence-free elements in 2D and 3D, though. In 2D, cf. Figure 1, we connect the barycenter of each triangle M in \tilde{T}_h to its three vertices.

The refined grid is called a Hsieh–Clough–Tocher grid (cf. [7, 12]):

$$\mathcal{T}_h = \{K_{M,i} \mid M = \cup_{i=1}^3 K_{M,i} \quad \forall M \in \tilde{\mathcal{T}}_h\}.$$

The P_2 - P_1^{dc} mixed finite element space for the 2D problem (2.1) is defined as follows, to be referred to as P_2 Hsieh–Clough–Tocher divergence-free element,

$$(2.2) \quad \mathbf{V}_h = \{ \mathbf{v}_h \in \mathbf{H}_0^1(\Omega) \mid \mathbf{v}_h|_K \in P_2(K)^2 \quad \forall K \in \mathcal{T}_h \},$$

$$(2.3) \quad P_h = \{ q_h \in L_0^2(\Omega) \mid q_h|_K \in P_1(K) \quad \forall K \in \mathcal{T}_h \}.$$

We note that when $\epsilon = 0$, \mathbf{V}_h in (2.2) should be enlarged by replacing the boundary condition $\mathbf{v}_h = \mathbf{0}$ with $\mathbf{v}_h \cdot \mathbf{n} = 0$:

$$(2.4) \quad \mathbf{V}_h = \{ \mathbf{v}_h \in \mathbf{C}(\Omega) \mid \mathbf{v}_h \cdot \mathbf{n}|_{\partial\Omega} = 0, \mathbf{v}_h|_K \in P_2(K)^2 \quad \forall K \in \mathcal{T}_h \},$$

$$(2.5) \quad P_h = \{ \operatorname{div} \mathbf{w}_h \mid \mathbf{w}_h \in \mathbf{V}_h \}.$$

The following uniform (in h) inf-sup condition is shown, via the macroelement technique of Stenberg [18], by Qin in [12]:

$$(2.6) \quad \inf_{q_h \in P_h} \sup_{\mathbf{v}_h \in \mathbf{V}_h} \frac{(q_h, \operatorname{div} \mathbf{v}_h)}{\|\mathbf{v}_h\|_{\mathbf{H}^1} \|q_h\|_{L^2}} \geq C.$$

However, we will show a stronger version inf-sup condition in this manuscript, for our singular perturbation problem (2.1), by constructing a divergence-preserving, polynomial-preserving, and boundary condition-preserving interpolation operator. For \mathbf{V}_h - P_h defined in (2.2)–(2.3), by the inf-sup condition (2.6), it follows that, i.e., (1.4) holds,

$$(2.7) \quad P_h = \operatorname{div} \mathbf{V}_h = \{ \operatorname{div} \mathbf{w}_h \mid \mathbf{w}_h \in \mathbf{V}_h \}.$$

(2.7) gives another definition for (2.3). For simplicity, (2.7) already is used in defining P_h above when $\epsilon = 0$. For any $q_h = \operatorname{div} \mathbf{w}_h \in P_h$, we have, by the divergence theorem,

$$\int_{\Omega} q_h \, d\mathbf{x} = \int_{\Omega} \operatorname{div} \mathbf{w}_h \, d\mathbf{x} = \int_{\partial\Omega} (\mathbf{w}_h \cdot \mathbf{n}) \, ds = 0,$$

as $\mathbf{w}_h \in \mathbf{V}_h \subset \mathbf{V}$. Here \mathbf{n} denotes the unit normal to $\partial\Omega$. Therefore, the mixed pair of finite element spaces is conforming:

$$(2.8) \quad \mathbf{V}_h \subset \mathbf{V}, \quad P_h \subset L_0^2.$$

Furthermore, the divergence-free finite element space is also a subspace of the continuous divergence-free space,

$$(2.9) \quad \mathbf{Z}_h \subset \mathbf{Z},$$

where

$$\mathbf{Z}_h = \{ \mathbf{v}_h \in \mathbf{V}_h \mid \operatorname{div} \mathbf{v}_h = 0 \} = \{ \mathbf{v}_h \in \mathbf{V}_h \mid \int_{\Omega} \operatorname{div} \mathbf{v}_h q_h \, d\mathbf{x} = 0 \quad \forall q_h \in P_h \},$$

$$\mathbf{Z} = \{ \mathbf{v} \in \mathbf{V} \mid \operatorname{div} \mathbf{v} = 0 \}.$$

The finite element approximation problem for (2.1) is then: Find $\mathbf{u}_h \in \mathbf{V}_h$ and $p \in P_h$ such that

$$(2.10) \quad \begin{aligned} a_{\epsilon}(\mathbf{u}_h, \mathbf{v}_h) - (p_h, \operatorname{div} \mathbf{v}_h) &= (\mathbf{f}, \mathbf{v}_h) \quad \forall \mathbf{v}_h \in \mathbf{V}_h, \\ (q_h, \operatorname{div} \mathbf{u}_h) &= (g, q_h) \quad \forall q_h \in P_h. \end{aligned}$$

3. Divergence-preserving interpolation. The main work is in this section: constructing an interpolation operator from \mathbf{H}_0^1 space to the discrete velocity space \mathbf{V}_h , which preserves the divergence. Such operators were constructed before by Girault and Scott [9] for Taylor–Hood elements and $(P_2 + B_3)$ - P_1 triangular elements. Straightforwardly, one would hope to interpolate a velocity $\mathbf{u} = \langle u_1, u_2 \rangle$ to preserve its gradient. But it is not possible. In general, it is not possible even to interpolate \mathbf{u} to preserve $\partial_x u_1$ and $\partial_y u_2$ only. Here, we preserve $\partial_x u_1 + \partial_y u_2$ pointwise in the sense of (1.5). As we are unable to prove the existence of such an \mathbf{I}_h abstractly, we give a constructive proof where the explicit dual basis functions are calculated. For example, instead of showing the invertibility of an 8×8 matrix A , we compute its inverse and list the entries in Figure 4.

The mixed finite element spaces \mathbf{V}_h and P_h in (2.2) and (2.3) are decomposed into global and local spaces:

$$\mathbf{V}_h = \tilde{\mathbf{V}}_h \oplus \bar{\mathbf{V}}_h, \quad P_h = \tilde{P}_h \oplus \bar{P}_h,$$

where

$$(3.1) \quad \tilde{\mathbf{V}}_h = \left\{ \mathbf{v}_h \in \mathbf{H}_0^1(\Omega) \mid \mathbf{v}_h|_M \in P_2(M) \quad \forall M \in \tilde{\mathcal{T}}_h \right\},$$

$$(3.2) \quad \bar{\mathbf{V}}_h = \left\{ \mathbf{v}_h \in \mathbf{V}_h \mid \mathbf{v}_h|_{\partial M} = 0 \quad \forall M \in \tilde{\mathcal{T}}_h \right\},$$

$$(3.3) \quad \tilde{P}_h = \left\{ q_h \in L_0^2(\Omega) \mid q_h|_M \in P_0(M) \quad \forall M \in \tilde{\mathcal{T}}_h \right\},$$

$$(3.4) \quad \bar{P}_h = \left\{ q_h \in P_h \mid \int_M q_h d\mathbf{x} = 0 \quad \forall M \in \tilde{\mathcal{T}}_h \right\}.$$

In other words, $\tilde{\mathbf{V}}_h$ is the C^0 - P_2 space on the original grid $\tilde{\mathcal{T}}_h$, $\bar{\mathbf{V}}_h$ is the space local macro- P_2 bubbles on each big triangle $M \in \tilde{\mathcal{T}}_h$ (which is refined into three triangles of \mathcal{T}_h), \tilde{P}_h is the traditional P_0^{dc} space on $\tilde{\mathcal{T}}_h$, and \bar{P}_h is the P_1^{dc} space of functions with mean value 0 on each macrotriangle M of the base grid $\tilde{\mathcal{T}}_h$. Here P_1^{dc} stands for the space of discontinuous, piecewise linear polynomials.

We define the divergence-preserving interpolation operator in two steps. First, we define an operator $\tilde{\mathbf{I}}_h$ from $\mathbf{H}_0^1(\Omega)$ to the subspace $\tilde{\mathbf{V}}_h$. This would be standard as described in [6], for example, if the function to be interpolated is slightly more regular than \mathbf{H}^1 so that its nodal values are well defined. To be general, we define $\tilde{\mathbf{I}}_h$ by the Scott–Zhang operator [16] which uses the edge averages as the nodal values of the interpolant so that the homogeneous boundary condition and polynomial functions are preserved. For each vertex \mathbf{x}_i of triangulation $\tilde{\mathcal{T}}_h$, we choose an edge $E_{\mathbf{x}_i}$ from $\tilde{\mathcal{T}}_h$ which is any one edge if \mathbf{x}_i is an internal vertex, or one boundary edge, cf. Figure 2,

$$(3.5) \quad E_{\mathbf{x}_i} \subset \partial\Omega \quad \text{if } \mathbf{x}_i \in \partial\Omega.$$

Let $\{\phi_{j,\mathbf{x}_i}(\mathbf{x}), j = 1, 2, 3\}$ be the three standard Lagrange P_2 nodal basis functions of $\tilde{\mathbf{V}}_h$ on the edge $E_{\mathbf{x}_i}$. In particular, ϕ_{1,\mathbf{x}_i} is numbered to be the P_2 nodal basis at the vertex \mathbf{x}_i . Then on the edge $E_{\mathbf{x}_i}$ we have a dual basis $\{\phi^{j,\mathbf{x}_i} \in P_2(E_{\mathbf{x}_i}), j = 1, 2, 3\}$ which is defined uniquely by

$$\int_{E_{\mathbf{x}_i}} \phi_{j,\mathbf{x}_i}(\mathbf{x}_s) \phi^{k,\mathbf{x}_i}(\mathbf{x}_s) ds = \begin{cases} 0 & \text{if } j \neq k, \\ 1 & \text{if } j = k. \end{cases}$$

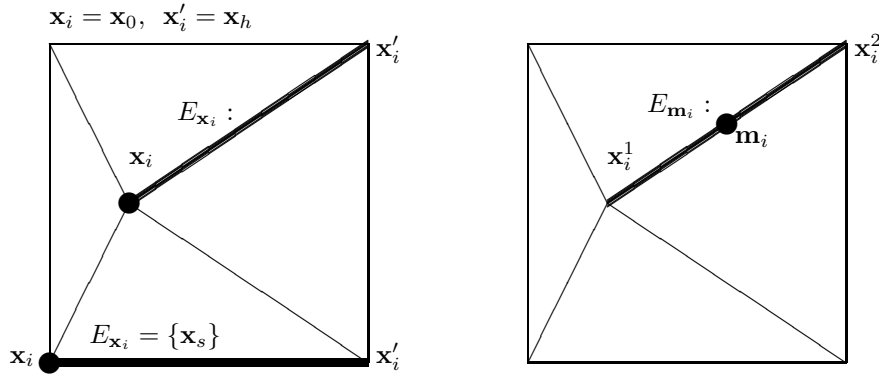


FIG. 2. Choose an edge for each $\tilde{\mathbf{V}}_h$ node, cf. (3.9) and (3.11).

In fact, it is easy to get that

$$(3.6) \quad \phi^{1,\mathbf{x}_i}(\mathbf{x}_s) = h^{-1} (30(s/h)^2 - 36(s/h) + 9),$$

$$(3.7) \quad \phi^{2,\mathbf{x}_i}(\mathbf{x}_s) = h^{-1} (-15(s/h)^2 + 15(s/h) - 3/2),$$

$$(3.8) \quad \phi^{3,\mathbf{x}_i}(\mathbf{x}_s) = h^{-1} (30(1 - s/h)^2 - 36(1 - s/h) + 9),$$

$$(3.9) \quad E_{\mathbf{x}_i} = \{\mathbf{x}_s = \mathbf{x}_i + (s/h)(\mathbf{x}'_i - \mathbf{x}_i) \mid 0 \leq s \leq h\},$$

where \mathbf{x}'_i is the other end point of edge $E_{\mathbf{x}_i}$, s is an arc-length parameter, and h is the length of the edge, cf. Figure 2. Therefore, we uniquely define the nodal value (a vector) of $\tilde{\mathbf{I}}_h \mathbf{v}$ for $\mathbf{v} \in \mathbf{H}_0^1(\Omega)$ at node \mathbf{x}_i :

$$(3.10) \quad (\tilde{\mathbf{I}}_h \mathbf{v})(\mathbf{x}_i) = \int_{E_{\mathbf{x}_i}} \mathbf{v}(\mathbf{x}_s) \phi^{1,\mathbf{x}_i}(\mathbf{x}_s) ds.$$

Next we define the midedge values of $\tilde{\mathbf{I}}_h \mathbf{v}(\mathbf{m}_i)$ so that the divergence of \mathbf{v} is preserved on each macrotriangle $M \in \tilde{\mathcal{T}}_h$. For each midedge point \mathbf{m}_i of grid $\tilde{\mathcal{T}}_h$, let $E_{\mathbf{m}_i}$ be the corresponding edge, cf. Figure 2. Using the same notations above, we let $\{\phi_{j,\mathbf{m}_i}(\mathbf{x}), j = 1, 2, 3\}$ be the three standard Lagrange P_2 nodal basis functions of $\tilde{\mathbf{V}}_h$ on the edge $E_{\mathbf{m}_i}$, where ϕ_{2,\mathbf{m}_i} is the P_2 nodal basis at the midpoint \mathbf{m}_i . We define, for each $\mathbf{v} \in \mathbf{H}_0^1(\Omega)$,

$$(3.11) \quad (\tilde{\mathbf{I}}_h \mathbf{v})(\mathbf{m}_i) = \frac{\int_{E_{\mathbf{m}_i}} (\mathbf{v}(\mathbf{x}_s) - (\tilde{\mathbf{I}}_h \mathbf{v})(\mathbf{x}_i^1) \phi_{1,\mathbf{x}_i^1}(\mathbf{x}_s) - (\tilde{\mathbf{I}}_h \mathbf{v})(\mathbf{x}_i^2) \phi_{1,\mathbf{x}_i^2}(\mathbf{x}_s)) \phi_{2,\mathbf{m}_i}(\mathbf{x}_s) ds}{\int_{E_{\mathbf{m}_i}} \phi_{2,\mathbf{m}_i}(\mathbf{x}_s) ds},$$

where \mathbf{x}_i^1 and \mathbf{x}_i^2 are the two end points of the edge $E_{\mathbf{m}_i}$, cf. Figure 2. Here (3.11) is well defined, as the integral in the denominator is nonzero.

LEMMA 3.1. *The following linear interpolation operator preserves the boundary condition, the $\tilde{\mathbf{V}}_h$ functions, and the divergence element-wise, and it is \mathbf{H}^1 -stable:*

$$(3.12) \quad \tilde{\mathbf{I}}_h \mathbf{v} = \sum_{\mathbf{x}_i \in \tilde{\mathcal{T}}_h} (\tilde{\mathbf{I}}_h \mathbf{v})(\mathbf{x}_i) \phi_{1,\mathbf{x}_i} + \sum_{\mathbf{m}_i \in \tilde{\mathcal{T}}_h} (\tilde{\mathbf{I}}_h \mathbf{v})(\mathbf{m}_i) \phi_{2,\mathbf{m}_i}, \quad \mathbf{v} \in \mathbf{H}_0^1(\Omega),$$

see (3.10) and (3.11). That is,

$$\begin{aligned} \tilde{\mathbf{I}}_h : \mathbf{H}_0^1(\Omega) &\rightarrow \tilde{\mathbf{V}}_h, & \tilde{\mathbf{I}}_h \mathbf{v}_h &= \mathbf{v}_h \quad \forall \mathbf{v}_h \in \tilde{\mathbf{V}}_h, \\ \int_M \operatorname{div} \tilde{\mathbf{I}}_h \mathbf{v} d\mathbf{x} &= \int_M \operatorname{div} \mathbf{v} d\mathbf{x} \quad \forall M \in \tilde{\mathcal{T}}_h, & \|\tilde{\mathbf{I}}_h \mathbf{v}\|_{\mathbf{H}^1} &\leq C \|\mathbf{v}\|_{\mathbf{H}^1}. \end{aligned}$$

Proof. Since we choose a boundary edge for each boundary vertex and for each midedge node on the boundary in (3.5), the averaged values are

$$(\tilde{\mathbf{I}}_h \mathbf{v})(\mathbf{x}_i) = \mathbf{0}, \quad (\tilde{\mathbf{I}}_h \mathbf{v})(\mathbf{m}_j) = \mathbf{0}, \quad \text{when } \mathbf{x}_i, \mathbf{m}_j \in \partial\Omega.$$

Hence $\tilde{\mathbf{I}}_h \mathbf{v}|_{\partial\Omega} = \mathbf{0}$ and $\tilde{\mathbf{I}}_h \mathbf{v} \in \tilde{\mathbf{V}}_h$. Next, the dual basis preserves the nodal values of P_2 polynomial at vertices, cf. (3.6)–(3.8); i.e.,

$$(3.13) \quad \tilde{\mathbf{I}}_h \mathbf{v}_h(\mathbf{x}_i) = \int_{E_{\mathbf{x}_i}} \phi^{1,\mathbf{x}_i} \left(\sum_{\mathbf{x}_j \in \tilde{\mathcal{T}}_h} \mathbf{v}_h(\mathbf{x}_j) \phi_{\mathbf{x}_j} + \sum_{\mathbf{m}_j \in \tilde{\mathcal{T}}_h} \mathbf{v}_h(\mathbf{m}_j) \phi_{\mathbf{m}_j} \right) ds = \mathbf{v}_h(\mathbf{x}_i).$$

At a midedge point \mathbf{m}_i , by (3.11) and (3.13), $\tilde{\mathbf{I}}_h \mathbf{v}_h(\mathbf{m}_i)$ is defined such that $\tilde{\mathbf{I}}_h \mathbf{v}_h = \mathbf{v}_h$ on the edge containing \mathbf{m}_i . Thus

$$(3.14) \quad \tilde{\mathbf{I}}_h \mathbf{v}_h(\mathbf{m}_i) = \mathbf{v}_h(\mathbf{m}_i).$$

On the other side, by the orthogonality of dual basis in (3.6)–(3.8), we have

$$\int_{E_{\mathbf{m}_i}} \phi^{2,\mathbf{m}_i} \left(\sum_{\mathbf{x}_j \in \tilde{\mathcal{T}}_h} \mathbf{v}_h(\mathbf{x}_j) \phi_{\mathbf{x}_j} + \sum_{\mathbf{m}_j \in \tilde{\mathcal{T}}_h} \mathbf{v}_h(\mathbf{m}_j) \phi_{\mathbf{m}_j} \right) ds = \mathbf{v}_h(\mathbf{m}_i) = \tilde{\mathbf{I}}_h \mathbf{v}_h(\mathbf{m}_i).$$

Thus we have, by (3.13) and (3.14),

$$\tilde{\mathbf{I}}_h \mathbf{v}_h = \mathbf{v}_h \quad \forall \mathbf{v}_h \in \tilde{\mathbf{V}}_h.$$

By mapping the dual basis to $[0, 1]$ and taking the averaging process on $[0, 1]$, it is straightforward to show the stability, cf. [16], that

$$\begin{aligned} \|\tilde{\mathbf{I}}_h \mathbf{v}\|_{\mathbf{H}^1(\Omega)}^2 &\leq \sum_{M \in \tilde{\mathcal{T}}_h} \left(\sum_{\mathbf{x}_i \in \tilde{\mathcal{T}}_h} (\tilde{\mathbf{I}}_h \mathbf{v})(\mathbf{x}_i)^2 \|\phi_{1,\mathbf{x}_i}\|_{\mathbf{H}^1(M)}^2 \right. \\ &\quad \left. + \sum_{\mathbf{m}_i \in \tilde{\mathcal{T}}_h} (\tilde{\mathbf{I}}_h \mathbf{v})(\mathbf{m}_i)^2 \|\phi_{2,\mathbf{m}_i}\|_{\mathbf{H}^1(M)}^2 \right) \\ &\leq C \sum_{\mathbf{x}_i \in \tilde{\mathcal{T}}_h} \|\phi^{1,\mathbf{x}_i}\|_{L^2(E_{\mathbf{x}_i})}^2 \|\mathbf{v}\|_{L^2(E_{\mathbf{x}_i})}^2 + C \sum_{\mathbf{m}_i \in \tilde{\mathcal{T}}_h} \|\phi^{2,\mathbf{m}_i}\|_{L^2(E_{\mathbf{m}_i})}^2 \|\mathbf{v}\|_{L^2(E_{\mathbf{m}_i})}^2 \\ &\leq C \sum_{\mathbf{x}_i \in \tilde{\mathcal{T}}_h} \|\mathbf{v}\|_{L^2(E_{\mathbf{x}_i})}^2 + C \sum_{\mathbf{m}_i \in \tilde{\mathcal{T}}_h} \|\mathbf{v}\|_{L^2(E_{\mathbf{m}_i})}^2 \\ (3.15) \quad &\leq C \sum_{M \in \tilde{\mathcal{T}}_h} \|\mathbf{v}\|_{L^2(M)} \|\mathbf{v}\|_{\mathbf{H}^1(M)} \leq C \|\mathbf{v}\|_{L^2(\Omega)} \|\mathbf{v}\|_{\mathbf{H}^1(\Omega)} \leq C \|\mathbf{v}\|_{\mathbf{H}^1(\Omega)}^2 \end{aligned}$$

for all $\mathbf{v} \in \mathbf{H}_0^1(\Omega)$.

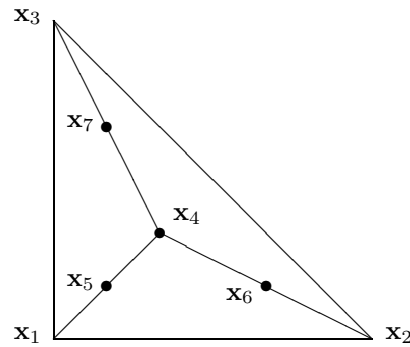


FIG. 3. The reference Hsieh-Clough-Tocher triangle and its nodes.

Finally, for element-wise divergence preserving, it follows by the divergence theorem and (3.11):

$$\begin{aligned}
 \int_M \operatorname{div}(\tilde{\mathbf{I}}_h \mathbf{v}) d\mathbf{x} &= \int_{\partial M} (\tilde{\mathbf{I}}_h \mathbf{v}) \cdot \mathbf{n} ds = \sum_{i=1}^3 \int_{E_{\mathbf{m}_i}} (\tilde{\mathbf{I}}_h \mathbf{v}) \cdot \mathbf{n}_i ds \\
 &= \sum_{i=1}^3 \int_{E_{\mathbf{m}_i}} \left([(\tilde{\mathbf{I}}_h \mathbf{v})(\mathbf{x}_i^1) \cdot \mathbf{n}_i] \phi_{\mathbf{x}_i^1} + [(\tilde{\mathbf{I}}_h \mathbf{v})(\mathbf{m}_i) \cdot \mathbf{n}_i] \phi_{\mathbf{m}_i} \right. \\
 &\quad \left. + [(\tilde{\mathbf{I}}_h \mathbf{v})(\mathbf{x}_i^2) \cdot \mathbf{n}_i] \phi_{\mathbf{x}_i^2} \right) ds \\
 &= \sum_{i=1}^3 \int_{E_{\mathbf{m}_i}} (\mathbf{v}(\mathbf{x}_s) \cdot \mathbf{n}_i) ds = \int_M \operatorname{div} \mathbf{v} d\mathbf{x}. \quad \square
 \end{aligned}$$

The second step in constructing the interpolation operator is to define the internal values for a piecewise P_2 function on a macro Hsieh-Clough-Tocher triangle, which consists of three triangles in \mathcal{T}_h . This is done first on the reference Hsieh-Clough-Tocher triangle, i.e., the unit right triangle at the origin, shown in Figure 3. We need to define eight internal nodal values of $(\mathbf{I}_h \mathbf{v})$. There are two components of $(\mathbf{I}_h \mathbf{v})$ at four internal P_2 nodes; see Figure 3. On the other side, there are precisely eight conditions to preserve the divergence of \mathbf{v} against P_h functions, since the dimension of the pressure space \bar{P}_h on one macro triangle is 8 (three P_1 functions would give a dimension of 9, but the condition of zero mean value would eliminate one dimension.) This is how Qin showed the inf-sup condition for the P_2 Hsieh-Clough-Tocher P_2 - P_1 divergence-free element in [12]. But we would build directly the interpolation operator by constructing explicitly a dual basis.

Let the internal nodes of C^0 - P_2 polynomials on the reference macrotriangle \hat{K} be numbered as in Figure 3, and $\{\hat{\phi}_i, i = 4, 5, 6, 7\}$ the four internal P_2 nodal basis functions. One such nodal basis function is plotted in Figure 5. Let A be the 8×8 matrix representing the vector semi- \mathbf{H}^1 inner product: its 2×2 blocks of 4×4 submatrices are $\int_{\hat{K}} \partial_l \hat{\phi}_i \partial_m \hat{\phi}_j d\hat{\mathbf{x}}, i, j = 4, 5, 6, 7, l, m = 1, 2$. By the analysis in [12], i.e., the inf-sup condition, it follows that A is invertible. But here we compute A^{-1} explicitly in order to construct a semi- \mathbf{H}^1 dual basis for the four vector nodal basis functions on \hat{K} . The entries of A^{-1} are displayed in Figure 4.

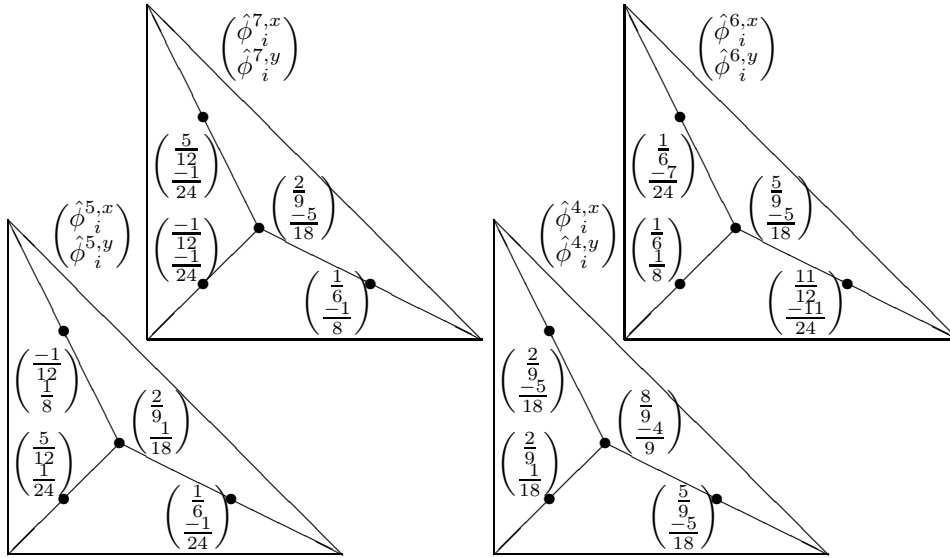


FIG. 4. The nodal values of semi- \mathbf{H}^1 dual basis, cf. (3.16) and Figure 5.

We define the dual basis $\hat{\mathbf{b}}^i(\mathbf{x}) = [\hat{b}_1^i(\hat{\mathbf{x}}), \hat{b}_2^i(\hat{\mathbf{x}})]$ by, cf. Figure 3 and Figure 4,

$$(3.16) \quad \hat{\mathbf{b}}^i(\hat{\mathbf{x}}) = \sum_{j=4}^7 \begin{pmatrix} \hat{\phi}_j^{i,x} \\ \hat{\phi}_j^{i,y} \end{pmatrix} \hat{\phi}_j(\hat{\mathbf{x}}), \quad i = 4, 5, 6, 7,$$

where the coefficients are displayed in Figure 4. Two such dual basis functions are depicted in Figure 5. One can verify that $\hat{\mathbf{b}}^i$ is a dual basis; i.e.,

$$(3.17) \quad \int_{\hat{K}} \frac{\partial \hat{\phi}_j}{\partial \hat{\mathbf{x}}}(\hat{\mathbf{x}}) \operatorname{div} \hat{\mathbf{b}}^i(\hat{\mathbf{x}}) d\hat{\mathbf{x}} = \delta_{ji}.$$

We note that we need only half of the matrix A^{-1} . In (3.16), the entries of the first four columns of A^{-1} are used. We may use the second four columns of A^{-1} to define another set of dual basis functions, then the partial directive in \hat{x} direction in (3.17) would be replaced by $\partial/\partial\hat{y}$ if the other dual basis is used. In fact, as the reference element is symmetric in \hat{x} and \hat{y} , by switching the two components of $\hat{\mathbf{b}}^i$, we would get the other set of dual basis functions. As we used the inverse matrix A^{-1} , we get immediately that

$$(3.18) \quad \int_{\hat{K}} \partial_{\hat{x}} \hat{\phi}_j (\partial_{\hat{x}} \hat{b}_1^i + \partial_{\hat{y}} \hat{b}_2^i) d\hat{\mathbf{x}} = \delta_{ij}, \quad \int_{\hat{K}} \partial_{\hat{y}} \hat{\phi}_j (\partial_{\hat{x}} \hat{b}_2^i + \partial_{\hat{y}} \hat{b}_1^i) d\hat{\mathbf{x}} = \delta_{ij}.$$

For a general triangle $M \in \tilde{\mathcal{T}}_h$, let $F : \hat{K} \rightarrow M$ be the reference mapping, known as Piola transformation ([6]); i.e.,

$$\mathbf{x} = F(\hat{\mathbf{x}}) = \sum_{j=1}^3 \mathbf{x}_j \bar{\phi}_j(\hat{\mathbf{x}}), \quad \hat{\mathbf{x}} \in \hat{K}, \quad \mathbf{x} \in M,$$

where \mathbf{x}_j are the three vertices of macrotriangle M and $\bar{\phi}_j$ are the P_1 nodal basis functions on \hat{K} . Let the Jacobian matrix and Jacobian of the affine transformation

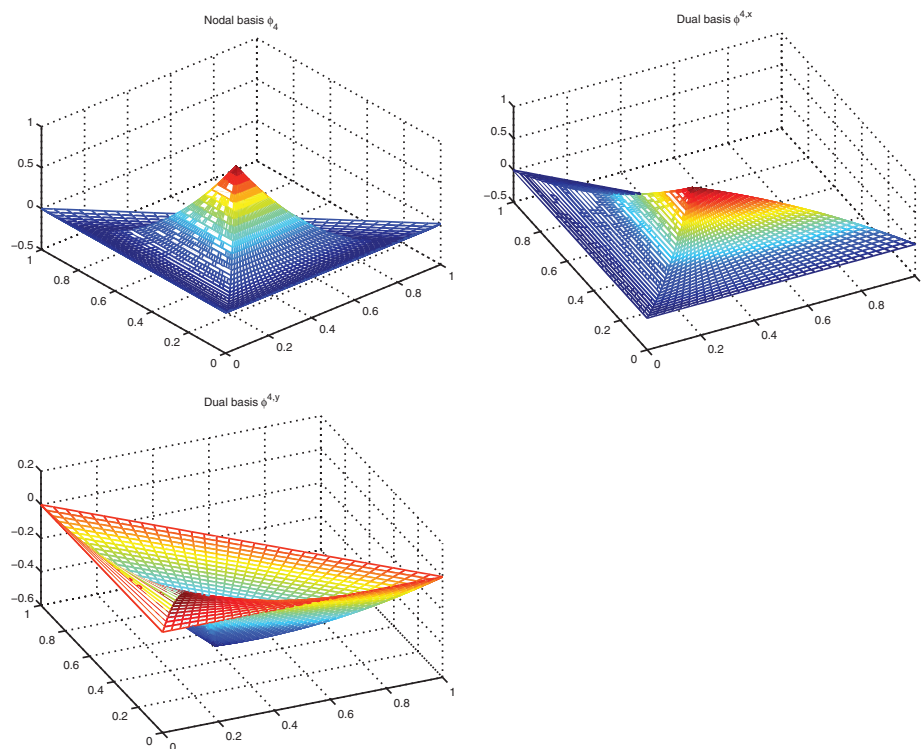


FIG. 5. A nodal basis and two dual basis functions, cf. (3.16).

F be, respectively,

$$(3.19) \quad T = \begin{pmatrix} \frac{\partial \mathbf{x}}{\partial \hat{\mathbf{x}}} \end{pmatrix} = \begin{pmatrix} t_{11} & t_{12} \\ t_{21} & t_{22} \end{pmatrix}, \quad J = \det(T).$$

In order to find the dual basis on M , we map the averaging integrals (3.18) on \hat{K} to integrals on M :

$$\begin{aligned} \delta_{ij} &= \int_{\hat{K}} \partial_{\hat{x}} \hat{\phi}_i (\partial_{\hat{x}} \hat{b}_1^j + \partial_{\hat{y}} \hat{b}_2^j) d\hat{\mathbf{x}} = \int_M (t_{11} \partial_x \phi_i + t_{21} \partial_y \phi_i) \\ &\quad (t_{11} \partial_x b_1^j + t_{21} \partial_y b_1^j + t_{12} \partial_x b_2^j + t_{22} \partial_y b_2^j) J^{-1} d\mathbf{x}, \\ 0 &= \int_{\hat{K}} \partial_{\hat{y}} \hat{\phi}_i (\partial_{\hat{x}} \hat{b}_1^j + \partial_{\hat{y}} \hat{b}_2^j) d\hat{\mathbf{x}} = \int_M (t_{12} \partial_x \phi_i + t_{22} \partial_y \phi_i) \\ &\quad (t_{11} \partial_x b_1^j + t_{21} \partial_y b_1^j + t_{12} \partial_x b_2^j + t_{22} \partial_y b_2^j) J^{-1} d\mathbf{x}, \\ \delta_{ij} &= \int_{\hat{K}} \partial_{\hat{y}} \hat{\phi}_i (\partial_{\hat{x}} \hat{b}_2^j + \partial_{\hat{y}} \hat{b}_1^j) d\hat{\mathbf{x}} = \int_M (t_{12} \partial_x \phi_i + t_{22} \partial_y \phi_i) \\ &\quad (t_{11} \partial_x b_2^j + t_{21} \partial_y b_2^j + t_{12} \partial_x b_1^j + t_{22} \partial_y b_1^j) J^{-1} d\mathbf{x}, \\ 0 &= \int_{\hat{K}} \partial_{\hat{x}} \hat{\phi}_i (\partial_{\hat{x}} \hat{b}_2^j + \partial_{\hat{y}} \hat{b}_1^j) d\hat{\mathbf{x}} = \int_M (t_{11} \partial_x \phi_i + t_{21} \partial_y \phi_i) \\ &\quad (t_{11} \partial_x b_2^j + t_{21} \partial_y b_2^j + t_{12} \partial_x b_1^j + t_{22} \partial_y b_1^j) J^{-1} d\mathbf{x}. \end{aligned}$$

Hence, we can linearly combine them to get

$$\begin{aligned} t_{22}\delta_{ij} &= \int_M \partial_x \phi_i [\partial_x(t_{11}b_1^j + t_{12}b_2^j) + \partial_y(t_{21}b_1^j + t_{22}b_2^j)] d\mathbf{x}, \\ -t_{12}\delta_{ij} &= \int_M \partial_y \phi_i [\partial_x(t_{11}b_1^j + t_{12}b_2^j) + \partial_y(t_{21}b_1^j + t_{22}b_2^j)] d\mathbf{x}, \\ -t_{21}\delta_{ij} &= \int_M \partial_x \phi_i [\partial_x(t_{11}b_2^j + t_{12}b_1^j) + \partial_y(t_{21}b_2^j + t_{22}b_1^j)] d\mathbf{x}, \\ t_{11}\delta_{ij} &= \int_M \partial_y \phi_i [\partial_x(t_{11}b_2^j + t_{12}b_1^j) + \partial_y(t_{21}b_2^j + t_{22}b_1^j)] d\mathbf{x}. \end{aligned}$$

Therefore, we conclude the calculation with the definition of the dual basis on M :

$$(3.20) \quad \mathbf{b}_{j,1}(\mathbf{x}) = \begin{pmatrix} \psi_{j,x}(\mathbf{x}) \\ \psi_{j,y}(\mathbf{x}) \end{pmatrix}, \quad \mathbf{b}_{j,2}(\mathbf{x}) = \begin{pmatrix} \psi_{j,y}(\mathbf{x}) \\ \psi_{j,x}(\mathbf{x}) \end{pmatrix},$$

where

$$(3.21) \quad \psi_{j,x}(\mathbf{x}) = \begin{cases} \frac{1}{t_{22}} \sum_{k=4}^7 \begin{pmatrix} t_{11}\hat{\phi}_k^{j,x} + t_{12}\hat{\phi}_k^{j,y} \\ t_{21}\hat{\phi}_k^{j,x} + t_{22}\hat{\phi}_k^{j,y} \end{pmatrix} \phi_k(\mathbf{x}), & \text{if } |t_{11}t_{22}| \geq J/2, \\ \frac{-1}{t_{21}} \sum_{k=4}^7 \begin{pmatrix} t_{12}\hat{\phi}_k^{j,x} + t_{11}\hat{\phi}_k^{j,y} \\ t_{22}\hat{\phi}_k^{j,x} + t_{21}\hat{\phi}_k^{j,y} \end{pmatrix} \phi_k(\mathbf{x}), & \text{if } |t_{11}t_{22}| < J/2, \end{cases}$$

$$(3.22) \quad \psi_{j,y}(\mathbf{x}) = \begin{cases} \frac{1}{t_{11}} \sum_{k=4}^7 \begin{pmatrix} t_{11}\hat{\phi}_k^{j,y} + t_{12}\hat{\phi}_k^{j,x} \\ t_{21}\hat{\phi}_k^{j,y} + t_{22}\hat{\phi}_k^{j,x} \end{pmatrix} \phi_k(\mathbf{x}), & \text{if } |t_{11}t_{22}| \geq J/2, \\ \frac{-1}{t_{12}} \sum_{k=4}^7 \begin{pmatrix} t_{12}\hat{\phi}_k^{j,y} + t_{11}\hat{\phi}_k^{j,x} \\ t_{22}\hat{\phi}_k^{j,y} + t_{21}\hat{\phi}_k^{j,x} \end{pmatrix} \phi_k(\mathbf{x}), & \text{if } |t_{11}t_{22}| < J/2, \end{cases}$$

where $\hat{\phi}_k^{j,x}$ and $\hat{\phi}_k^{j,y}$ are defined in Figure 4, cf. Figure 3. The second step in constructing the interpolation operator is

$$(3.23) \quad \begin{aligned} \bar{\mathbf{I}}_h : \mathbf{H}_0^1(\Omega) &\rightarrow \bar{\mathbf{V}}_h, \\ \bar{\mathbf{I}}_h : \mathbf{v} = \begin{pmatrix} v_1 \\ v_2 \end{pmatrix} &\mapsto \sum_{K \in \bar{\Omega}} \sum_{j=4}^7 (\bar{\mathbf{I}}_h \mathbf{v})(\mathbf{x}_j) \phi_j(\mathbf{x}), \\ (\bar{\mathbf{I}}_h \mathbf{v})(\mathbf{x}_j) &= \int_K \begin{pmatrix} \partial_x v_1(\mathbf{x}) \operatorname{div} \mathbf{b}_{j,1}(\mathbf{x}) \\ \partial_y v_2(\mathbf{x}) \operatorname{div} \mathbf{b}_{j,2}(\mathbf{x}) \end{pmatrix} d\mathbf{x}, \end{aligned}$$

where $\bar{\mathbf{V}}_h$ is defined in (3.2) and $\mathbf{b}_{j,i}$ are defined by (3.20)–(3.22).

THEOREM 3.1. *The following linear, \mathbf{H}^1 -stable interpolation operator preserves the boundary condition, the \mathbf{V}_h finite element functions, and the divergence inside the finite element space \mathbf{V}_h :*

$$(3.24) \quad \mathbf{I}_h \mathbf{v} = \tilde{\mathbf{I}}_h \mathbf{v} + \bar{\mathbf{I}}_h(\mathbf{v} - \tilde{\mathbf{I}}_h \mathbf{v}), \quad \mathbf{v} \in \mathbf{H}_0^1(\Omega),$$

where $\tilde{\mathbf{I}}_h$ and $\bar{\mathbf{I}}_h$ are defined in (3.12) and (3.23), respectively.

Proof. The idea is to use the eight degrees of freedom of $\mathbf{I}_h \mathbf{v}$ inside each macrotriangle $M \in \tilde{\mathcal{T}}_h$, cf. Figure 3, to match the eight nodal values of $P_0 \operatorname{div}(\mathbf{v} - \tilde{\mathbf{I}}_h \mathbf{v})$, where P_0 is the L^2 -orthogonal projector to P_h . Note that each linear P_1^{dc} function in P_h has

3×3 coefficients on a macrotriangle M which consists of three triangles. But $\operatorname{div} \tilde{\mathbf{I}}_h \mathbf{v}$ matches the mean value of $\operatorname{div} \mathbf{v}$ on M so that $P_0 \operatorname{div}(\mathbf{v} - \tilde{\mathbf{I}}_h \mathbf{v})$ has 8 independent coefficients.

Since the support of $\tilde{\mathbf{I}}_h \mathbf{v}$ is inside each macrotriangle K of $\tilde{\mathcal{T}}_h$, \mathbf{I}_h preserves the homogeneous boundary condition of \mathbf{v} , by Lemma 3.1. For any $\mathbf{v}_h \in \mathbf{V}_h$, by Lemma 3.1, $(\tilde{\mathbf{I}}_h \mathbf{v}_h - \mathbf{v}_h) \in \tilde{\mathbf{V}}_h$, defined in (3.2); i.e., $(\tilde{\mathbf{I}}_h \mathbf{v}_h - \mathbf{v}_h) = 0$ on ∂M for all $M \in \tilde{\mathcal{T}}_h$. Let

$$(\mathbf{v}_h - \tilde{\mathbf{I}}_h \mathbf{v}_h)(\mathbf{x}) = \sum_{M \in \tilde{\mathcal{T}}_h} \sum_{j=4}^7 (\mathbf{v}_h - \tilde{\mathbf{I}}_h \mathbf{v}_h)(\mathbf{x}_j) \phi_j(\mathbf{x}) = \sum_{M \in \tilde{\mathcal{T}}_h} \sum_{j=4}^7 \begin{pmatrix} C_{M,j} \\ D_{M,j} \end{pmatrix} \phi_j(\mathbf{x}),$$

for some constants $C_{M,j}$ and $D_{M,j}$. Now, inside each triangle $M \in \tilde{\mathcal{T}}_h$, by (3.21) and (3.22),

$$\begin{aligned} \tilde{\mathbf{I}}_h(\mathbf{v}_h - \tilde{\mathbf{I}}_h \mathbf{v}_h)(\mathbf{x}_i) &= \int_M \sum_{j=4}^7 \begin{pmatrix} C_{M,j} \partial_x \phi_j(\mathbf{x}) \operatorname{div} \mathbf{b}_{i,1}(\mathbf{x}) \\ D_{M,j} \partial_y \phi_j(\mathbf{x}) \operatorname{div} \mathbf{b}_{i,2}(\mathbf{x}) \end{pmatrix} d\mathbf{x} \\ (3.25) \qquad \qquad \qquad &= \begin{pmatrix} C_{M,i} \\ D_{M,i} \end{pmatrix} = \mathbf{v}_h(\mathbf{x}_i) - \tilde{\mathbf{I}}_h \mathbf{v}_h(\mathbf{x}_i), \end{aligned}$$

for $i = 4, 5, 6, 7$. That is, $\tilde{\mathbf{I}}_h$ is an identity operator on $(\mathbf{v}_h - \tilde{\mathbf{I}}_h \mathbf{v}_h)$. Hence,

$$(3.26) \qquad \mathbf{I}_h \mathbf{v}_h = \tilde{\mathbf{I}}_h \mathbf{v}_h + \tilde{\mathbf{I}}_h(\mathbf{v}_h - \tilde{\mathbf{I}}_h \mathbf{v}_h) = \tilde{\mathbf{I}}_h \mathbf{v}_h + (\mathbf{v}_h - \tilde{\mathbf{I}}_h \mathbf{v}_h) = \mathbf{v}_h.$$

Next, for showing the divergence preserving, we need to notice that for any $\bar{q}_h \in \bar{P}_h$, there is a $\bar{\mathbf{w}}_h \in \bar{\mathbf{V}}_h$, cf. (3.2) and (3.4), such that

$$(3.27) \qquad \operatorname{div} \bar{\mathbf{w}}_h = \bar{q}_h.$$

To show (3.27) on each element $M \in \tilde{\mathcal{T}}_h$, we map M to the reference element \hat{K} . As the matrix A for defining the dual basis is invertible, on \hat{K} , $\{\operatorname{div} \bar{\mathbf{w}}_h|_M\}$ is an 8-dimensional subspace of \bar{P}_h restricted on M . On the other side, the dimension of itself, \bar{P}_h restricted on M , is 8. So (3.27) holds. Then, as $\{\mathbf{b}_{j,1}, \mathbf{b}_{j,2}\}$ form a basis for $\bar{\mathbf{V}}_h$ restricted on each M , we have the following linear combination, cf. (3.20) and (3.22):

$$(3.28) \qquad \bar{\mathbf{w}}_h = \sum_{M \in \tilde{\mathcal{T}}_h} \sum_{j=4}^7 w_1^{M,j} \mathbf{b}_{j,1}(\mathbf{x}) + w_2^{M,j} \mathbf{b}_{j,2}(\mathbf{x}).$$

In fact, the coefficients $w_i^{M,j}$ in (3.28) can easily be found by (3.25) and (3.21)–(3.22), as $\tilde{\mathbf{I}}_h \bar{\mathbf{w}}_h = \bar{\mathbf{w}}_h$. For all $\mathbf{v} \in \mathbf{H}_0^1(\Omega)$ and $\mathbf{w}_h \in \mathbf{V}_h$, denoting $\operatorname{div} \mathbf{w}_h = \tilde{q}_h \oplus \bar{q}_h$ for some

$\tilde{q}_h \in \tilde{P}_h$ and $\bar{q}_h = \operatorname{div} \bar{\mathbf{w}}_h \in \bar{P}_h$, we have, by Lemma 3.1 and (3.28),

$$\begin{aligned} & \int_{\Omega} \operatorname{div}(\mathbf{v} - \mathbf{I}_h \mathbf{v}) \operatorname{div} \mathbf{w}_h \, d\mathbf{x} \\ &= \int_{\Omega} \operatorname{div}(\mathbf{v} - \tilde{\mathbf{I}}_h \mathbf{v}) \operatorname{div} \mathbf{w}_h \, d\mathbf{x} - \int_{\Omega} \sum_{M \in \tilde{\mathcal{T}}_h} \sum_{j=4}^7 \left(c_{M,j,1} \partial_x \phi_j(\mathbf{x}) + c_{M,j,2} \partial_y \phi_j(\mathbf{x}) \right) \operatorname{div} \mathbf{w}_h \, d\mathbf{x} \\ &= \int_{\Omega} \operatorname{div}(\mathbf{v} - \tilde{\mathbf{I}}_h \mathbf{v}) \bar{q}_h \, d\mathbf{x} - \int_{\Omega} \sum_{M \in \tilde{\mathcal{T}}_h} \sum_{j=4}^7 \left(c_{M,j,1} \partial_x \phi_j(\mathbf{x}) + c_{M,j,2} \partial_y \phi_j(\mathbf{x}) \right) \operatorname{div} \bar{\mathbf{w}}_h \, d\mathbf{x} \\ &= \int_{\Omega} \operatorname{div}(\mathbf{v} - \tilde{\mathbf{I}}_h \mathbf{v}) \bar{q}_h \, d\mathbf{x} - \sum_{M \in \tilde{\mathcal{T}}_h} \sum_{i=4}^7 \sum_{j=4}^7 \left(c_{M,j,1} \int_M \partial_x \phi_j(\mathbf{x}) w_1^{M,i} \operatorname{div} \mathbf{b}_{i,1}(\mathbf{x}) \, d\mathbf{x} \right. \\ & \qquad \qquad \qquad \left. + c_{M,j,2} \int_M \partial_y \phi_j(\mathbf{x}) w_2^{M,i} \operatorname{div} \mathbf{b}_{i,2}(\mathbf{x}) \, d\mathbf{x} \right) \\ &= \int_{\Omega} \operatorname{div}(\mathbf{v} - \tilde{\mathbf{I}}_h \mathbf{v}) \bar{q}_h \, d\mathbf{x} - \sum_{M \in \tilde{\mathcal{T}}_h} \sum_{j=4}^7 \left(c_{M,j,1} w_1^{M,j} + c_{M,j,2} w_2^{M,i} \right), \end{aligned}$$

where

$$\begin{pmatrix} c_{M,j,1} \\ c_{M,j,2} \end{pmatrix} = \bar{\mathbf{I}}_h(\mathbf{v} - \tilde{\mathbf{I}}_h \mathbf{v})(\mathbf{x}_j) = \begin{pmatrix} \int_M \partial_x(\mathbf{v} - \tilde{\mathbf{I}}_h \mathbf{v})_1(\mathbf{y}) \operatorname{div} \mathbf{b}_{j,1}(\mathbf{y}) \, d\mathbf{y} \\ \int_M \partial_y(\mathbf{v} - \tilde{\mathbf{I}}_h \mathbf{v})_2(\mathbf{y}) \operatorname{div} \mathbf{b}_{j,2}(\mathbf{y}) \, d\mathbf{y} \end{pmatrix}.$$

Hence,

$$\begin{aligned} & \int_{\Omega} \operatorname{div}(\mathbf{v} - \mathbf{I}_h \mathbf{v}) \operatorname{div} \mathbf{w}_h \, d\mathbf{x} \\ &= \int_{\Omega} \operatorname{div}(\mathbf{v} - \tilde{\mathbf{I}}_h \mathbf{v}) \bar{q}_h \, d\mathbf{x} - \sum_{M \in \tilde{\mathcal{T}}_h} \sum_{j=4}^7 \left(\int_M \partial_x(\mathbf{v} - \tilde{\mathbf{I}}_h \mathbf{v})_1(\mathbf{y}) \operatorname{div} \mathbf{b}_{j,1}(\mathbf{y}) \, d\mathbf{y} w_1^{M,j} \right. \\ & \qquad \qquad \qquad \left. + \int_M \partial_y(\mathbf{v} - \tilde{\mathbf{I}}_h \mathbf{v})_2(\mathbf{y}) \operatorname{div} \mathbf{b}_{j,2}(\mathbf{y}) \, d\mathbf{y} w_2^{M,j} \right) \\ &= \int_{\Omega} \operatorname{div}(\mathbf{v} - \tilde{\mathbf{I}}_h \mathbf{v}) \bar{q}_h \, d\mathbf{x} - \int_{\Omega} \operatorname{div}(\mathbf{v} - \tilde{\mathbf{I}}_h \mathbf{v}) \operatorname{div} \bar{\mathbf{w}}_h \, d\mathbf{x} = 0. \end{aligned}$$

Finally, by mapping $\mathbf{I}_h \mathbf{v}$ to the reference element, the same way in proving (3.15), it is standard to show the stability that $\|\mathbf{I}_h \mathbf{v}\|_{\mathbf{H}^1} \leq C \|\mathbf{v}\|_{\mathbf{H}^1}$ for all $\mathbf{v} \in \mathbf{H}_0^1(\Omega)$, cf. [16]. \square

4. The convergence analysis. We will show that the divergence-free element solution is the best approximation in the finite element subspaces, under appropriate norms, to the exact solutions of the Darcy–Stokes–Brinkman system (2.1), uniformly for $\epsilon \in [0, 1]$.

Following [10], the following parameter-dependent norm is introduced for the analysis:

$$(4.1) \qquad \qquad \qquad \|\mathbf{u}\|_{\epsilon}^2 = a_{\epsilon}(\mathbf{u}, \mathbf{u}) + (\operatorname{div} \mathbf{u}, \operatorname{div} \mathbf{u}) \quad \forall \mathbf{u} \in \mathbf{V}.$$

When $\epsilon = 1$, $\|\cdot\|_{\epsilon}$ is equivalent to the \mathbf{H}^1 -norm and equivalent to the $\mathbf{H}^{\operatorname{div}}$ -norm when $\epsilon = 0$. We show the inf-sup condition again with respect this ϵ -dependent norm in the next lemma.

LEMMA 4.1. *Both bilinear forms are coercive:*

$$(4.2) \quad a_\epsilon(\mathbf{z}_h, \mathbf{z}_h) \geq \|\mathbf{z}_h\|_\epsilon^2 \quad \forall \mathbf{z}_h \in \mathbf{Z}_h,$$

$$(4.3) \quad \sup_{\mathbf{v}_h \in \mathbf{V}_h} \frac{(\operatorname{div} \mathbf{v}_h, q_h)}{\|\mathbf{v}_h\|_\epsilon} \geq C \|q_h\|_{L^2} \quad \forall q_h \in P_h.$$

Proof. We note that (4.2) holds in fact as an equality by (2.9) and (4.1). This is a difficult point in other finite element methods for the Darcy–Stokes–Brinkman system, cf. [10, 19]. But it becomes trivial for our \mathbf{H}^1 -conforming, divergence-free element.

For (4.3), cf. [13, 2], there is a $\mathbf{v} \in H_0^1(\Omega)^d$ such that

$$\operatorname{div} \mathbf{v} = q_h \quad \text{and} \quad \|\mathbf{v}\|_{\mathbf{H}^1} \leq C \|q_h\|_{L^2}.$$

Let $\mathbf{v}_h = \mathbf{I}_h \mathbf{v}$. By Theorem 3.1, we get

$$\operatorname{div} \mathbf{v}_h = q_h$$

and consequently the inf-sup condition

$$\frac{(\operatorname{div} \mathbf{v}_h, q_h)}{\|q_h\|_{L^2}} = \|q_h\|_{L^2} \geq C \|\mathbf{v}\|_{\mathbf{H}^1} \geq C \|\mathbf{v}_h\|_{\mathbf{H}^1} \geq \sqrt{\frac{C}{1+\epsilon}} \|\mathbf{v}_h\|_\epsilon. \quad \square$$

We are ready to show the main theory, the quasioptimality of the Hsieh–Clough–Tocher P_2 divergence-free element.

THEOREM 4.1. *Let the solution in the Darcy–Stokes–Brinkman system (2.1) be (\mathbf{u}, p) such that $(\mathbf{u}, p) \in (\mathbf{V}, L_0^2)$ when $\epsilon > 0$, and $(\mathbf{u}, p) \in (\mathbf{V} \cap \mathbf{H}^1, L_0^2)$ when $\epsilon = 0$. Let \mathbf{V}_h and P_h be defined in (2.2) and (2.3), respectively, if $\epsilon > 0$, or in (2.4) and (2.5), respectively, if $\epsilon = 0$. The finite element solutions in (2.10) approximate (\mathbf{u}, p) optimally,*

$$(4.4) \quad \begin{aligned} & \|\operatorname{div}(\mathbf{u} - \mathbf{u}_h)\|_{L^2} = \inf_{q_h \in P_h} \|\operatorname{div} \mathbf{u} - q_h\|_{L^2}, \\ & \|\mathbf{u} - \mathbf{u}_h\|_\epsilon + \|p - p_h\|_{L^2} \leq C \left(\inf_{\mathbf{v}_h \in \mathbf{V}_h} \|\mathbf{u} - \mathbf{v}_h\|_\epsilon + \inf_{q_h \in P_h} \|p - q_h\|_{L^2} \right). \end{aligned}$$

Further, if the solution (\mathbf{u}, p) is regular with some $0 < r \leq 2$ in (2.1),

$$(4.5) \quad \|\operatorname{div}(\mathbf{u} - \mathbf{u}_h)\|_{L^2} \leq Ch^r \|\mathbf{u}\|_{\mathbf{H}^{r+1}},$$

$$(4.6) \quad \|\mathbf{u} - \mathbf{u}_h\|_\epsilon + \|p - p_h\|_{L^2} \leq Ch^r (\epsilon |\mathbf{u}|_{\mathbf{H}^{r+1}} + |\mathbf{u}|_{\mathbf{H}^r} + |p|_{H^r}).$$

Proof. The proof below carries through for both $\epsilon \in (0, 1]$ and $\epsilon = 0$.

By the inf-sup condition, there is a unique solution (\mathbf{u}_h, p_h) :

$$(4.7) \quad a_\epsilon(\mathbf{u} - \mathbf{u}_h, \mathbf{v}_h) - (p - p_h, \operatorname{div} \mathbf{v}_h) = 0 \quad \forall \mathbf{v}_h \in \mathbf{V}_h,$$

$$(4.8) \quad (q_h, \operatorname{div}(\mathbf{u} - \mathbf{u}_h)) = 0 \quad \forall q_h \in P_h.$$

By the second equation, we get the best approximation for the divergence:

$$(4.9) \quad \|\operatorname{div}(\mathbf{u} - \mathbf{u}_h)\|_{L^2}^2 = (\operatorname{div} \mathbf{u} - q_h, \operatorname{div}(\mathbf{u} - \mathbf{u}_h)) \leq \|\operatorname{div} \mathbf{u} - q_h\|_{L^2} \|\operatorname{div}(\mathbf{u} - \mathbf{u}_h)\|_{L^2},$$

$$(4.10) \quad \|\operatorname{div}(\mathbf{u} - \mathbf{u}_h)\|_{L^2} = \inf_{q_h \in P_h} \|\operatorname{div} \mathbf{u} - q_h\|_{L^2}.$$

Let $P_0 p$ be the L^2 orthogonal projection of the pressure p in space P_h ; i.e., $(q_h, P_0 p) = (q_h, p)$ for all $q_h \in P_h$. By (4.8), we have

$$(4.11) \quad (P_0 p - p_h, \operatorname{div}(\mathbf{u} - \mathbf{u}_h)) = 0.$$

Since $(q_h, \operatorname{div}(\mathbf{u} - \mathbf{I}_h \mathbf{u})) = 0$, shown in Theorem 3.1, we get

$$(P_0 p - p_h, \operatorname{div}(\mathbf{I}_h \mathbf{u} - \mathbf{u}_h)) = 0.$$

Letting $\mathbf{v}_h = (\mathbf{I}_h \mathbf{u} - \mathbf{u}_h) \in \mathbf{V}_h$ in (4.7), we get

$$(4.12) \quad a_\epsilon(\mathbf{u} - \mathbf{u}_h, \mathbf{I}_h \mathbf{u} - \mathbf{u}_h) = 0.$$

Using the Cauchy–Schwarz inequality, we get the following estimates for the velocity

$$(4.13) \quad \begin{aligned} \|\mathbf{u} - \mathbf{u}_h\|_\epsilon^2 &= a_\epsilon(\mathbf{u} - \mathbf{u}_h, \mathbf{u} - \mathbf{I}_h \mathbf{u}) \leq \|\mathbf{u} - \mathbf{u}_h\|_\epsilon \|\mathbf{u} - \mathbf{I}_h \mathbf{u}\|_\epsilon, \\ \|\mathbf{u} - \mathbf{u}_h\|_\epsilon &\leq \|\mathbf{u} - \mathbf{I}_h \mathbf{u}\|_\epsilon. \end{aligned}$$

For the pressure approximation, we have

$$(4.14) \quad \|p - p_h\|_{L^2} \leq \|p - P_0 p\|_{L^2} + \|P_0 p - p_h\|_{L^2}.$$

As Ω is a 2D Lipschitz domain, by the continuous inf-sup condition, i.e., the maximal right inverse of the divergence operator, cf. [13, 2], there is a $\mathbf{v} \in \mathbf{H}_0^1(\Omega)$ such that

$$\operatorname{div} \mathbf{v} = P_0 p - p_h \quad \text{and} \quad \|\mathbf{v}\|_{\mathbf{H}^1} \leq C \|P_0 p - p_h\|_{L^2}.$$

Let $\mathbf{v}_h = \mathbf{I}_h \mathbf{v}$ in (4.7). By the preservation of divergence of \mathbf{I}_h in Theorem 3.1, we get

$$\begin{aligned} \|P_0 p - p_h\|_{L^2}^2 &= a_\epsilon(\mathbf{u} - \mathbf{u}_h, \mathbf{I}_h \mathbf{v}) \leq \|\mathbf{u} - \mathbf{u}_h\|_\epsilon (\epsilon \|\mathbf{I}_h \mathbf{v}\|_{\mathbf{H}^1} + \|\mathbf{I}_h \mathbf{v}\|_{L^2}) \\ &\leq \|\mathbf{u} - \mathbf{u}_h\|_\epsilon \|\mathbf{I}_h \mathbf{v}\|_{\mathbf{H}^1} \leq C \|\mathbf{u} - \mathbf{u}_h\|_\epsilon \|\mathbf{v}\|_{\mathbf{H}^1} \\ &\leq C \|\mathbf{u} - \mathbf{u}_h\|_\epsilon \|P_0 p - p_h\|_{L^2}. \end{aligned}$$

Thus, by (4.14), (4.13), and Theorem 3.1, we get

$$(4.15) \quad \begin{aligned} \|p - p_h\|_{L^2} &\leq \|p - P_0 p\|_{L^2} + C \|\mathbf{u} - \mathbf{u}_h\|_\epsilon \\ &\leq \inf_{q_h \in P_h} \|p - q_h\|_{L^2} + C \inf_{\mathbf{v}_h \in \mathbf{V}_h} \|\mathbf{u} - \mathbf{v}_h\|_\epsilon. \quad \square \end{aligned}$$

Normally, the solution of (1.1) depends on ϵ . So as ϵ approaches zero, the convergence estimates given in Theorem 4.1 will be deteriorate, especially in the case that the solution of (1.1) has boundary layers. Let

$$H_+^1 = \left\{ g \in H^1 \cap L_0^2 \mid \int_\Omega \frac{|g(x)|^2}{|x - x_j|^2} dx < \infty, \quad j = 1, 2, \dots, N \right\}$$

with the norm

$$\|g\|_{1,+}^2 = \|g\|_1^2 + \sum_{j=1}^N \int_\Omega \frac{|g(x)|^2}{|x - x_j|^2} dx,$$

where x_1, x_2, \dots, x_N denote the vertices of polygonal domain Ω . We assume the domain Ω and the data in (1.1) are regular enough so that the solutions of (1.1) satisfy

$$(4.16) \quad \begin{aligned} \epsilon^2 \|\mathbf{u}\|_{\mathbf{H}^2} + \epsilon \|\mathbf{u}\|_{\mathbf{H}^1} + \|\mathbf{u} - \mathbf{u}^0\|_{L^2} + \|p - p^0\|_{H^1} + \\ \epsilon^{\frac{1}{2}} \|\mathbf{u}^0\|_{\mathbf{H}^1} + \epsilon^{\frac{1}{2}} \|p^0\|_{H^1} \leq C \epsilon^{\frac{1}{2}} (\|\mathbf{f}\|_{\mathbf{H}^{\operatorname{curl}1}} + \|g\|_{1,+}), \end{aligned}$$

where (\mathbf{u}^0, p^0) is the solution of (1.1) when $\epsilon = 0$. (4.16) is proved in [10] for convex polygonal domain Ω , using the regularity results of [2]. Applying the same techniques developed in [10], we have the following uniform convergence estimate. We note that, compared to the convergence rate in Theorem 4.1 (assuming there the regularity constant $r = 1$), we lose half an order of convergence, shown in next theorem. Nevertheless, the rate for the divergence remains optimal by (4.5) of Theorem 4.1.

THEOREM 4.2. *Let \mathbf{V}_h and P_h be defined in (2.2) and (2.3), respectively. If (4.16) holds, then there is a constant C , independent of ϵ , such that*

$$(4.17) \quad \|\mathbf{u} - \mathbf{u}_h\|_{\mathbf{L}^2} + \epsilon \|\mathbf{curl}(\mathbf{u} - \mathbf{u}_h)\|_{\mathbf{L}^2} + \|p - p_h\|_{L^2} \leq Ch^{1/2}(\|\mathbf{f}\|_{\mathbf{H}^{\mathbf{curl}}} + \|g\|_{1,+}).$$

Proof. We repeat the proof in [10] with Theorem 3.1. By (4.4) and (4.16), we get

$$\begin{aligned} \|\mathbf{u} - \mathbf{u}_h\|_{\mathbf{L}^2} &\leq C\|\mathbf{u} - \mathbf{I}_h\mathbf{u}\|_{\mathbf{L}^2} \leq C\|(\mathbf{I} - \mathbf{I}_h)(\mathbf{u} - \mathbf{u}^0)\|_{\mathbf{L}^2} + C\|(\mathbf{I} - \mathbf{I}_h)\mathbf{u}^0\|_{\mathbf{L}^2} \\ &\leq Ch^{1/2}(\|\mathbf{u} - \mathbf{u}^0\|_{\mathbf{L}^2}^{1/2}\|\mathbf{u} - \mathbf{u}^0\|_{\mathbf{H}^1}^{1/2} + h^{1/2}\|\mathbf{u}^0\|_{\mathbf{H}^1}) \\ &\leq Ch^{1/2}(\|\mathbf{f}\|_{\mathbf{H}^{\mathbf{curl}}} + \|g\|_{1,+}). \end{aligned}$$

By (4.4), (4.5), and (4.16),

$$\begin{aligned} \epsilon\|\mathbf{curl}(\mathbf{u} - \mathbf{u}_h)\|_{\mathbf{L}^2} &\leq C\epsilon\|\mathbf{u} - \mathbf{I}_h\mathbf{u}\|_{\mathbf{H}^1} \leq C\epsilon h^{1/2}\|\mathbf{u}\|_{\mathbf{H}^1}^{1/2}\|\mathbf{u}\|_{\mathbf{H}^2}^{1/2} \\ &\leq Ch^{1/2}(\|\mathbf{f}\|_{\mathbf{H}^{\mathbf{curl}}} + \|g\|_{1,+}). \end{aligned}$$

Finally, by (4.15), (4.16), and the two estimates above, it follows that

$$\begin{aligned} \|p - p_h\|_{L^2} &\leq \|p - P_0 p\|_{L^2} + C\|\mathbf{u} - \mathbf{u}_h\|_{\epsilon} \\ &\leq Ch\|p - p^0\|_{H^1} + Ch\|p^0\|_{H^1} + C\|\mathbf{u} - \mathbf{u}_h\|_{\epsilon} \\ &\leq Ch^{1/2}(\|\mathbf{f}\|_{\mathbf{H}^{\mathbf{curl}}} + \|g\|_{1,+}). \quad \square \end{aligned}$$

5. Numerical tests. We apply the Hsieh–Clough–Tocher P_2 divergence-free element to two model problems of Darcy–Stokes–Brinkman equations, where one is regular while the other has a boundary layer. The numerical results confirm the analysis for both cases. We continue to apply the method to a channel flow problem where the viscosity has a big jump.

We repeat the computation for a model problem in [10]. We solve (1.1) on the unit square $\Omega = (0, 1)^2$ with the exact solution:

$$(5.1) \quad \mathbf{u} = \mathbf{curl} \sin^2(\pi x_1) \sin^2(\pi x_2) = \pi \begin{pmatrix} \sin^2(\pi x_1) \sin(2\pi x_2) \\ -\sin^2(\pi x_2) \sin(2\pi x_1) \end{pmatrix},$$

$$(5.2) \quad p = \sin(\pi x_1) - \frac{2}{\pi}.$$

That is, $g = 0$ in (1.1) and

$$\mathbf{f} = (1 + 4\epsilon^2\pi^2)\mathbf{u} + 2\epsilon^2\pi^3 \begin{pmatrix} \cos(2\pi x_1) \sin(2\pi x_2) \\ -\cos(2\pi x_2) \sin(2\pi x_1) \end{pmatrix} - \begin{pmatrix} \pi \cos(\pi x_1) \\ 0 \end{pmatrix}.$$

We take a sequence of uniform grids on the domain Ω as the base grids. Then each base grid is refined into a Hsieh–Clough–Tocher grid by connecting the barycenter of each triangle to the three vertices. Three levels of computational grids are shown in Figure 6. We define multilevel finite element spaces \mathbf{V}_h and P_h ((2.2) and (2.3)) on

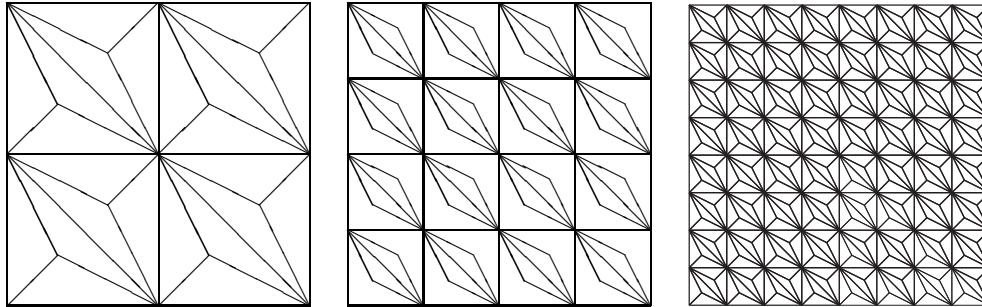


FIG. 6. The level 3, 4, and 5 Hsieh-Clough-Tocher grid \mathcal{T}_h in Table 1.

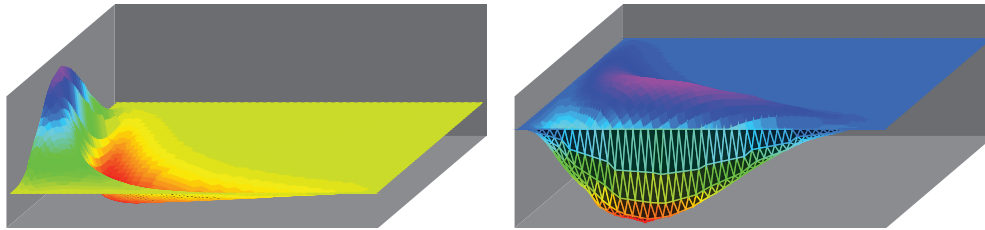
TABLE 1
The errors and orders of convergence for P_2 HCT divergence-free element.

Level	$\ \mathbf{e}_u\ _{l^\infty}$	h^n	$\ \mathbf{e}_u\ _{L^2}$	h^n	$\ \mathbf{e}_u\ _{\mathbf{H}^1}$	h^n	$\ e_p\ _{l^\infty}$	h^n	$\ e_p\ _{L^2}$	h^n
$\epsilon = 1$ in (2.10)										
3	1.75780	—	1.11846	—	13.53769	—	53.55211	—	18.50145	—
4	0.32259	2.4	0.18254	2.6	4.51836	1.6	31.45767	0.8	8.16259	1.2
5	0.04646	2.8	0.02586	2.8	1.44821	1.6	12.24402	1.4	3.39324	1.3
6	0.00603	2.9	0.00316	3.0	0.42560	1.8	3.71159	1.7	1.19218	1.5
$\epsilon = e^{-1}$ in (2.10)										
3	1.72846	—	1.10515	—	13.54040	—	13.94648	—	4.78990	—
4	0.31621	2.5	0.17821	2.6	4.51816	1.6	7.93903	0.8	2.05655	1.2
5	0.04583	2.8	0.02531	2.8	1.44822	1.6	3.06569	1.4	0.84939	1.3
6	0.00596	2.9	0.00312	3.0	.42560	1.8	0.92926	1.7	0.29811	1.5
$\epsilon = 4^{-2}$ in (2.10)										
3	1.62753	—	1.06127	—	13.57410	—	4.01395	—	1.35218	—
4	0.29508	2.5	0.16490	2.7	4.52095	1.6	2.05128	1.0	0.52846	1.3
5	0.04368	2.8	0.02364	2.8	1.44842	1.6	0.77066	1.4	0.21333	1.3
6	0.00594	2.9	0.00299	3.0	0.42560	1.8	0.23366	1.7	0.07458	1.5
$\epsilon = 4^{-4}$ in (2.10)										
3	1.44164	—	0.88100	—	14.53164	—	0.72949	—	0.22448	—
4	0.27507	2.4	0.11814	2.9	4.62103	1.7	0.18672	2.0	0.04422	2.3
5	0.03917	2.8	0.01814	2.7	1.45392	1.7	0.05206	1.8	0.01426	1.6
6	0.00590	2.7	0.00257	2.8	0.42580	1.8	0.01641	1.7	0.00474	1.6
$\epsilon = 0$ in (2.10)										
3	1.55194	—	0.83451	—	16.83536	—	0.41060	—	0.12466	—
4	0.29178	2.4	0.10507	3.0	4.91961	1.8	0.04987	3.0	0.01088	3.5
5	0.04053	2.8	0.01628	2.7	1.49852	1.7	0.00876	2.5	0.00209	2.3
6	0.00594	2.8	0.00243	2.7	0.43134	1.8	0.00188	2.2	0.00050	2.0

such Hsieh-Clough-Tocher grids. For the resulting linear systems of equations (2.10), we solve them by the iterated penalty method, cf. [8, 6, 5, 17].

In Table 1, we list the errors of finite element solutions in various norms and the convergence orders for the solutions. They seem to be of optimal order in convergence, confirming the theory in Theorem 4.1. That is, order 3 for the velocity solutions in maximum norm and in L^2 norm while order 2 in \mathbf{H}^1 norm and order 2 for the pressure solutions in maximum and L^2 norms. These orders of convergence are independent of the perturbation parameter ϵ because the solutions are regular here, independent of ϵ .

Next, we apply the Hsieh-Clough-Tocher P_2 divergence-free element to the Darcy-Stokes-Brinkman equations where the solutions are not regular, i.e., with boundary

FIG. 7. The exact solution \mathbf{u} of test problem (5.3) with boundary layers.TABLE 2
The P_2 divergence-free HCT element for test problem (5.3).

Level	$\ \mathbf{e}_u\ _{L^2}$	h^n	$\ \mathbf{e}_u\ _{\mathbf{H}^1}$	h^n	$\ e_p\ _{L^2}$	h^n
$\epsilon = 1$ in (5.3)						
2	1.0892		12.01		24.23	
3	0.9074	0.26	11.09	0.12	15.86	0.61
4	0.1697	2.42	4.16	1.41	9.11	0.79
5	0.0223	2.93	1.31	1.67	3.56	1.35
6	0.0026	3.12	0.37	1.84	1.17	1.61
$\epsilon = 4^{-1}$ in (5.3)						
2	0.6322		6.696		4.124	
3	0.5535	0.19	7.822		2.957	0.47
4	0.1263	2.13	3.426	1.19	1.888	0.64
5	0.0168	2.90	1.098	1.64	0.875	1.10
6	0.0019	3.08	0.304	1.84	0.553	0.66
$\epsilon = 4^{-2}$ in (5.3)						
2	0.1634		2.584		0.9806	
3	0.2300		4.106		0.5823	0.75
4	0.1078	1.09	3.610	0.18	0.4875	0.25
5	0.0218	2.30	1.767	1.03	0.3750	0.37
6	0.0033	2.72	0.580	1.60	0.3363	0.15
$\epsilon = 4^{-4}$ in (5.3)						
2	1.9040		36.87		3.0790	
3	0.9475	1.00	19.08	0.95	1.2450	1.30
4	0.4342	1.12	12.17	0.64	0.5166	1.26
5	0.1798	1.27	5.82	1.06	0.2123	1.28
6	0.0723	1.31	2.40	1.27	0.1035	1.03

layers. We solve (1.1) on the unit square $\Omega = (0, 1)^2$ with the exact solution:

$$(5.3) \quad \mathbf{u} = \mathbf{curl} f_1, \quad p = \epsilon(1 - e^{-1/\epsilon}) - e^{-x_1/\epsilon},$$

where

$$f_1 = 2^8 e^{-x_1 x_2 / \epsilon} x_1^2 (1 - x_1)^2 x_2^2 (1 - x_2)^2.$$

That is, $g = 0$ in (1.1) and

$$\mathbf{f} = (1 - \epsilon \Delta) \mathbf{u} - \mathbf{grad} p.$$

We note that the two components of \mathbf{u} have each a boundary layer in each direction, shown in Figure 7.

Compared to the convergence orders in Table 1, we can see that we lose some orders of convergence here in Table 2. However, the errors and the orders of convergence shown in Table 2 are consistent with the theory shown in Theorem 4.2.

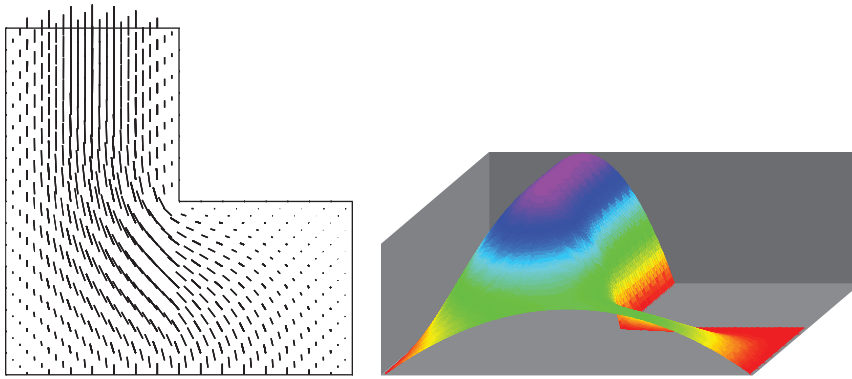


FIG. 8. The \mathbf{u}_h field and the second component of \mathbf{u}_h , cf. (5.4).

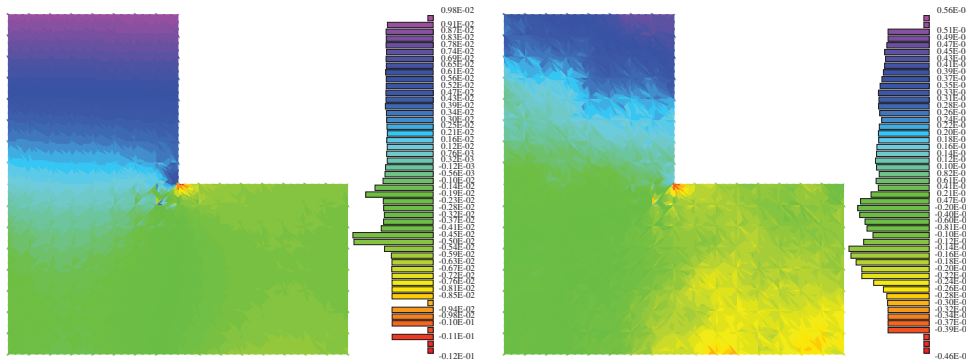


FIG. 9. p_h plots for $\epsilon = 1$ and $\epsilon = 4^{-4}$, cf. (5.4).

Our third numerical test is on computing a flow driven by a boundary force, not by an internal force, i.e., for the problem (1.1) where $\mathbf{f} = 0, g = 0$, but $\mathbf{u}|_{\partial\Omega} \neq 0$. The domain is shown in Figure 8, where the inflow and outflow boundary condition are, respectively,

$$(5.4) \quad \mathbf{u}(x, 0) = \begin{pmatrix} 0 \\ x(2-x) \end{pmatrix}, \quad \mathbf{u}(x, 2) = \begin{pmatrix} 0 \\ 8x(1-x) \end{pmatrix}.$$

In Figure 8, we plot the computed velocity field \mathbf{u}_h and the second component of \mathbf{u}_h for $\epsilon = 1$ in (1.1). The corresponding graphs for $\epsilon = 4^{-4}$ are nearly identical. In Figure 9, the computed pressure p_h is shown for $\epsilon = 1$ and $\epsilon = 4^{-4}$. They are slightly different.

Acknowledgment. We thank the anonymous referees for their helpful comments and suggestions.

REFERENCES

[1] D.N. ARNOLD AND J. QIN, *Quadratic velocity/linear pressure Stokes elements*, in *Advances in Computer Methods for Partial Differential Equations VII*, R. Vichnevetsky and R.S. Steplemen, eds., IMACS, Elsevier, Amsterdam, 1992.
 [2] D. ARNOLD, L.R. SCOTT, AND M. VOGELIUS, *Regular inversion of the divergence operator with Dirichlet conditions on a polygon*, *Ann. Sc. Norm. Super. Pisa, C1. Sci. (5)*, 15 (1988), pp. 169–192.

- [3] G. BAKER, W. JUREIDINI, AND A. KARAKASHIAN, *Piecewise solenoidal vector fields and the Stokes problem*, SIAM J. Numer. Anal., 27 (1990), pp. 1466–1485.
- [4] B. BERNSTEIN, K.A. FEIGL, AND T. OLSEN, *A first-order exactly incompressible finite element for axisymmetric fluid flow*, SIAM J. Numer. Anal., 33 (1996), pp. 1736–1758.
- [5] S.C. BRENNER AND L.R. SCOTT, *The Mathematical Theory of Finite Element Methods*, Springer-Verlag, New York, 1994.
- [6] F. BREZZI AND M. FORTIN, *Mixed and Hybrid Finite Element Methods*, Springer-Verlag, New York, 1991.
- [7] P.G. CIARLET, *The Finite Element Method for Elliptic Problems*, North-Holland, Amsterdam, 1978.
- [8] M. FORTIN AND R. GLOWINSKI, *Augmented Lagrangian Methods: Applications to the Numerical Solution of Boundary-Value Problems*, North-Holland, Amsterdam, 1983.
- [9] V. GIRAULT AND L.R. SCOTT, *A quasi-local interpolation operator preserving the discrete divergence*, Calcolo, 40 (2003), pp. 1–19.
- [10] K.A. MARDAL, X.-C. TAI, AND R. WINTHER, *A robust finite element method for Darcy–Stokes flow*, SIAM J. Numer. Anal., 40 (2002), pp. 1605–1631.
- [11] D.A. NIELD AND A. BEJAN, *Convection in Porous Media*, Springer-Verlag, New York, 2006.
- [12] J. QIN, *On the convergence of some low order mixed finite elements for incompressible fluids*, Thesis, Pennsylvania State University, University Park, PA, 1994.
- [13] P.A. RAVIART AND V. GIRAULT, *Finite Element Methods for Navier-Stokes Equations*, Springer-Verlag, New York, 1986.
- [14] L.R. SCOTT AND M. VOGELIUS, *Norm estimates for a maximal right inverse of the divergence operator in spaces of piecewise polynomials*, RAIRO, Modelisation Math. Anal. Numer., 19 (1985), pp. 111–143.
- [15] L.R. SCOTT AND M. VOGELIUS, *Conforming finite element methods for incompressible and nearly incompressible continua*, in Lectures in Applied Mathematics 22, B.E. Engquist, S. Osher, and R.C.J. Somerville, eds., AMS, Providence, RI, 1985, pp. 221–244.
- [16] L.R. SCOTT AND S. ZHANG, *Finite element interpolation of nonsmooth functions satisfying boundary conditions*, Math. Comp., 54 (1990), pp. 483–493.
- [17] L.R. SCOTT AND S. ZHANG, *Multilevel iterated penalty method for mixed elements*, in Domain Decomposition Methods in Sciences and Engineering, PE. Bjorstad, M.S. Espedal, and D.E. Keyes, eds., Domain Decomposition Press, Bergen, Norway, 1998, pp. 133–139.
- [18] R. STENBERG, *Analysis of mixed finite element methods for the Stokes problem: A unified approach*, Math. Comp., 42 (1984), pp. 9–23.
- [19] X.P. XIE, J.C. XU, AND G.R. XUE, *Uniformly-stable finite element methods for Darcy-Stokes-Brinkman models*, J. Comput. Math., 26 (2008), pp. 437–455.
- [20] S. ZHANG, *A new family of stable mixed finite elements for 3D Stokes equations*, Math. Comp., 74 (2005), pp. 543–554.
- [21] S. ZHANG, *On the P1 Powell-Sabin divergence-free finite element for the Stokes equations*, J. Comput. Math., 26 (2008), pp. 456–470.
- [22] S. ZHANG, *A family of $Q_{k+1,k} \times Q_{k,k+1}$ divergence-free finite elements on rectangular grids*, SIAM J. Numer. Anal., 47 (2009), pp. 2090–2107.